Journal of Colloid and Interface Science **250,** 400–408 (2002)
doi:10.1006/jcis.2002.8317

Advective Flow and Floc Permeability

G. W. Tsou,* R. M. Wu,* P. S. Yen,* D. J. Lee,*[,1] and X. F. Peng†

Department of Chemical Engineering, National Taiwan University, Taipei, Taiwan, 106, Republic of China; and †Thermal Engineering Department, Tsinghua University, Beijing, 100084, China

Received August 20, 2001; accepted February 21, 2002; published online May 15, 2002

This work monitored advection flow through a floc by bubble tracking. Close examination of the motion of a swarm of hydrogen bubbles that passed over a free-falling floc allowed the extent of advection flow to be estimated at 53% for the original activated sludge floc, and 12% for the flocculated floc. The interior permeability of the sludge flocs was estimated from this information. The fluid force exerted on the falling floc was also considered. © 2002 Elsevier Science (USA)

Key Words: **advection; permeability; floc; hydrodynamic drag.**

INTRODUCTION

As widely assumed, a sludge floc is a porous fractal-like aggregate that consists of many primary particles (1–4). The flocs generated in the treatment of water and wastewater usually have a fractal dimension between 1.4 and 2.8 (1). Physical and chemical treatment may affect the floc's structure, and thus, the corresponding density and fractal dimension (5, 6).

The hydrodynamic drag force on a floc must be thoroughly understood to predict its motion. This force on a floc depends on many factors, including the drag coefficient (7), primary particle density (5), and the correction factor for advection flow (8, 9). Lee *et al*. (10) reviewed the current state of understanding of this issue. The floc permeability, k, must be known *a priori* to determine the correction factor. Masliyah and Polikar (11) experimentally determined the terminal velocities and interior permeabilities of artificial, porous spheres. Logan and Hunt (12) reported a significant influence of aggregate permeability on the advection flow through a floc. Moreover, Li and Ganczarczyk (9) established the existence of advection flow using a settling test. However, the structure of floc is very fragile and tends to break down under shearing, explaining why the floc interior permeability cannot be precisely evaluated by the conventional column test (which is performed in a filled column with through-flowing liquid). Empirical models in the literature typically assess the floc's permeability. For example, Matsumoto *et al*. (13) used Davies' correlation to estimate the floc's permeability. Li and Ganczarczyk (3) compared the permeability determined by the Carman–Kozeny equation with that determined by Davies' correlation. Huang (7) used Brinkman's model to estimate permeability. Lee *et al*. (10) considered six popular permeability models to estimate the floc's interior permeability. Rogak and Flagan (14) also suggested a permeability expression based on the fractal nature of a floc. The permeability of floc, estimated according to various works, differs by two to three orders of magnitude.

Wu *et al*. (15) applied a hydrodynamic approach to estimate the permeability of the floc's interior. The basic concept is simple: the response of a porous floc subjected to a (mild) change in its hydrodynamic environment should differ from that of a nonporous object of the same size and weight. The floc's interior permeability can be estimated by comparing the movements of various flocs. Wu *et al*. observed the motion of porous floc moving toward an impermeable plate and compared it to that of a nonporous sphere, thereby estimating the floc's interior permeability in waste-activated sludge. The permeabilities of polymer-flocculated sludge flocs and fluid-sheared flocs were estimated accordingly (16, 17). The advection flow through the floc's interior influences the capture of fine particles by the floc (18).

Although most literature that addressed floc processes assumes a significant advection flow, no direct, experimental evidence of such a flow is available. Therefore, the validity of the advection flow-based works cited above cannot be considered justified. Saleh *et al*. (19) performed particle image velocimetry (PIV) to monitor the fluid field along porous media, from which salient characteristics of fluid flow at a porous boundary had been evaluated. This work used bubble-tracking to observe directly the advection flow and the nearby flow-around fluid field of a sludge floc. The radius of the "fluid tube" that flowed through the floc was determined first, after then the floc's permeability was estimated following an approach briefly summarized below.

CAPTURE RATIO AND FLOC PERMEABILITY

Consider a porous sphere of radius, R, falling freely in an infinitely large pool of Newtonian fluid. Under the sphere exists a fluid tube of radius ω, while the fluid within the tube would

[1] To whom correspondence should be addressed. Fax: 886-2-2362-3040. E-mail: djlee@ccms.ntu.edu.tw.

0021-9797/02 $35.00

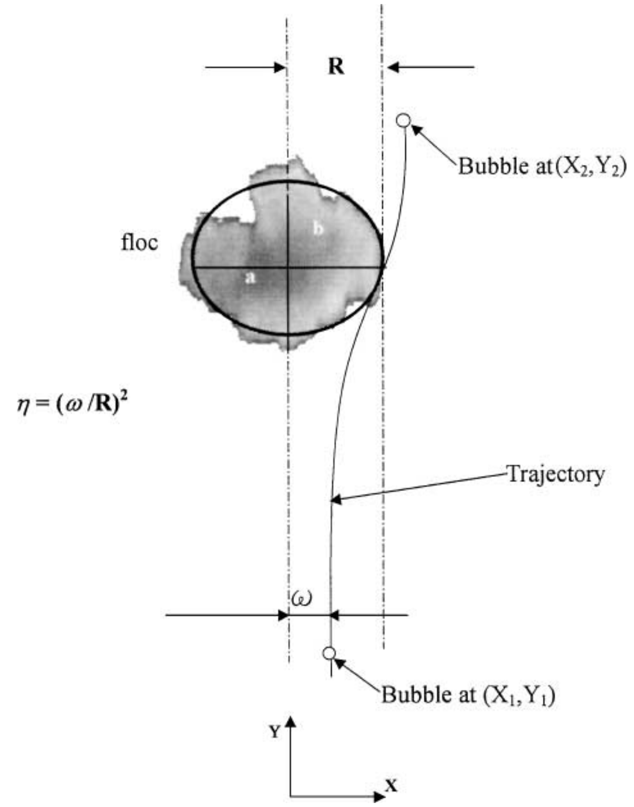

FIG. 1. Schematics of the falling floc and the rising bubbles. *a* and *b* are the two diameters of the floc. The demonstrated bubble has a trajectory that just swept-over the floc surface.

flow through the sphere. Outside this tube, the fluid flows around the sphere (Fig. 1). Clearly, no fluid can flow through an impermeable sphere with $\omega/R = 0$. At the other extreme, at the "no sphere" limit, or for a sphere with infinitely large permeability, $\omega/R \rightarrow 1.0$, and the fluid can directly flow through the sphere. For a porous sphere of permeability k, ω/R ranges between zero and unity, depending on the ease with which the fluid flows through the sphere. As Fig. 1 shows, the fluid particles originating at position (X_1, Y_1) just sweep over the sphere's surface at position (X_2, Y_2). Estimating the dimensionless permeability depends on estimating the dimensionless ratio, ω/R.

Assuming the Brinkman model of the interior of the sphere and the creeping flow condition, Adler (20) derived the analytical solution for the ratio ω/R as a function of the dimensionless scale $\beta = R/k^{0.5}$, as

$$\left(\frac{\omega}{R}\right)^2 = \eta = 1 - \frac{c}{\beta} - \frac{d}{\beta}, \quad [1]$$

where

$$c = -\frac{1}{J}\left[(\beta^5 + 6\beta^3)\left(1 - \frac{\tanh\beta}{\beta}\right)\right], \quad [2a]$$

$$d = \frac{3\beta^3}{J}\left[\left(1 - \frac{\tanh\beta}{\beta}\right)\right], \quad [2b]$$

$$J = 2\beta^2 + 3 - \frac{3\tanh\beta}{\beta}. \quad [2c]$$

Apparently, η can be considered to be the capture ratio of the sphere and is a function of β only. Therefore, if the η value can be experimentally assessed, then the corresponding β value can be obtained by Eq. [1].

Bubble tracking was used here to estimate the capture ratio of the sludge flocs. A swarm of bubbles was released from the bottom of a pool and rose along the centerline of the falling floc. The bubbles basically follow the streamline of the fluid because they are small (typically under 5 μm in diameter). Observing the interaction between the floc and the bubbles yields useful information about the fluid field and the capture ratio, and thus allows the permeability of the floc to be estimated. Tracing the streamline that just sweeps over the floc surface at (X_1, Y_1) and the one that is far away from the sphere at (X_2, Y_2) allows the ω and the R values to be estimated, and thus determines the β value. Apparently, all bubbles are expelled from the floc if most of the approaching fluid fails to flow through the floc (impermeable floc in which the advection flow is negligible). At the other extreme all the approaching bubbles directly penetrate the floc without distorting its direction of motion, if the floc interior was void (the "no sphere" limit). Finally, for a partially permeable floc, some of the approaching bubbles would be expelled and the remainder would penetrate the floc.

EXPERIMENTAL

A waste-activated sludge sample was taken from the wastewater treatment plant, the Neili Bread Plant of the Presidental Enterprise Co. in Taoyuan, Taiwan, and was tested within two hours after sampling. Data concerning chemical oxygen demand (COD), suspended solids (SS), and turbidity were obtained for the supernatant drawn from the sludge, using EPA Taiwan standard methods. The results were 5.6 mg/L (COD), 7.1 mg/L (SS), and 1.4 NTU (turbidity). The weight percentage of the sludge sample was 0.7% (w/w). The solid density of the sludges was measured using an Accupyc Pycnometer 1330 (Micromeritics) to be 1.450 kg/m^3. The zeta meter (Zetasizer 200, Marlvern) measured the zeta potential of the original sludge flocs at −16 mV. Cationic flocculant, T-3052 from Kai-Kuan Corp., Taiwan, was used to condition the sludge. Cationic polyelectrolyte flocculant, polymer T-3052, was obtained from Kai-Guan Inc., Taiwan. The polymer T-3052 is a cationic polyacrylamide with a mean molecular weight of 10^7 and a charge density of 20%. The mixing unit was a baffled mixing chamber with a stirrer. The weighed sludge was first placed in the mixing chamber, and the polymer solution was slowly poured in and stirred at 200 rpm for 5 min, and then at 50 rpm for another 20 min.

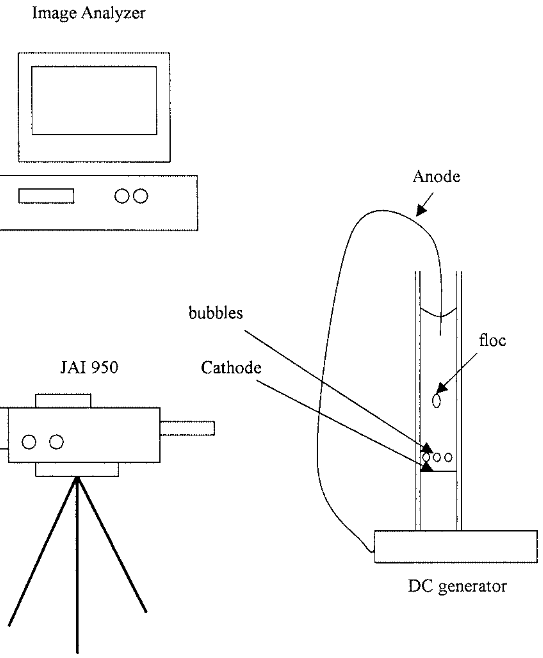

FIG. 2. Schematics of the testing assembly.

Figure 2 schematically depicts the testing apparatus. A glass tank (10 cm (L) × 10 cm (W) × 30 cm (H)) was used to examine floc-settling. A floc was carefully released from the top of the column and settled at a terminal velocity of V_i. Two plates with central holes were placed in the settling tube to screen out the flocs that did not move along the central line. A platinum wire of diameter 35 μm was hung across the centerline, close to the bottom of the tank, as the cathode. This cathode was connected to a pulse generator (Bubble Generator, MN-305, Sugawara, Japan). The anode was near the top of the tank, and therefore did not interfere with the floc's motion. The pulse generator produced electrical pulses every 5 ms, and thus gave chains of tiny hydrogen bubbles from the cathode. Two digital cameras, JAI 950 1/3″ (JAI, 210 pixels per mm) and NEC TC-22A (130 pixels per mm), both equipped with a close-up lens (MML2-110D) recorded the floc's motion. The images were continuously sent to a workstation for processing. The entire alignment was adjusted to the display in the observation window, the point at which the settling floc and the rising bubble chains met.

The images were analyzed using the software, Inspector V2.2 (Matrox). The cross-sectional area of the floc was recorded, along with the Feret diameters along the horizontal (F_x) and vertical (F_y) axes. The center of the floc was fixed at the OR point midway between the two Feret diameters. Data on the positions of the floc's center versus time enables the settling velocity of floc (V_f) to be estimated using numerical smoothing and differentiation. The centers and sizes of the rising bubbles were determined from the cross-sectional area and the centers of mass. Identifying the center of the floc and rising bubbles enabled their individual moving velocities ($\mathbf{V}_f$ and $\mathbf{V}_b$ values) to be determined as functions of time.

RESULTS AND DISCUSSION

Advection Flow through the Floc

Figure 3 displays a portion of the microphotographs of the original floc A1 (diameter 985 μm) during its interaction with the rising bubbles. The floc's interior is rather loose and transparent. The terminal velocity of floc A1, before it interacts with the rising bubbles, is 0.13 mm/s, giving a Reynolds number of 0.13.

Figure 3a shows the falling floc and a few rising bubbles from the first bubble chain. The bubbles, indicated by the arrow, are located just beneath the floc. These bubbles, when far away from the floc, show a rising terminal velocity of 0.13 mm/s. In Fig. 3b, which was recorded 0.42 s after Fig. 3a, the indicated bubbles have moved into the floc and are trapped there, indicating that the floc's interior is indeed highly permeable and fluid can flow through it (advection flow). Hence, the hypothesis of the existence of advection flow is, for the first time, justified. Thereafter, in Figs. 3c and 3d, more bubbles penetrate the floc. The arrow shows the same bubble as discussed above. The floc starts to move *upward* rather than *downward* because of the added buoyancy force caused by the increased number of trapped bubbles (Fig. 3e).

Experimental observations revealed that the response of most original sludge flocs, when interacting with rising bubbles, resembles that of the floc, A1. However, the interior of a few original flocs is very dense. Figure 4 shows such a case. The original floc, A4 (diameter of 1430 μm), interacts with the rising bubbles, as it settles. Evidently, the interior of A4 is considerably denser than that of A1. Furthermore, the V_t of A4 is 1.18 mm/s, which is nine times higher than that of A1, despite the former being only 50% larger than the latter. According to Fig. 4a, the falling floc and the rising bubbles approach each other. The bubble indicated by the arrow approaches the floc at a relative velocity of 3.89 mm/s. In Fig. 4b, which shows the situation 0.42 s after Fig. 4a, the falling floc falls at a velocity near its undisturbed terminal velocity, V_t. The velocity of the indicated bubbles, meanwhile, declines. Subsequently, as Figs. 4c and 4d reveal, the indicated bubble is "pushed down" by the falling floc. Restated, unlike for A1, the bubbles below the floc A4 do not penetrate the floc but are pushed downward, revealing that the advection flow is minimized since the interior of floc, A4, is dense.

Figure 5 shows the response of a typical flocculated floc, P4 (diameter of 1.310 μm), as it interacts with rising bubbles. Experimental observation showed that the response of most flocculated sludge flocs resembles that of floc P4. Apparently, the interior of P4 is denser than that of floc A1, but looser than that of floc A4. V_t of P4 is 2.48 mm/s, which is 18 times greater than that of A1. Figure 5a depicts the falling floc and the rising bubbles. The bubbles indicated by the arrow approach the floc at a velocity of 0.92 mm/s. In Fig. 5b, the falling floc falls at a velocity close to its terminal velocity. Some bubbles penetrate the floc while the other is pushed away (Figs. 5c–5e).

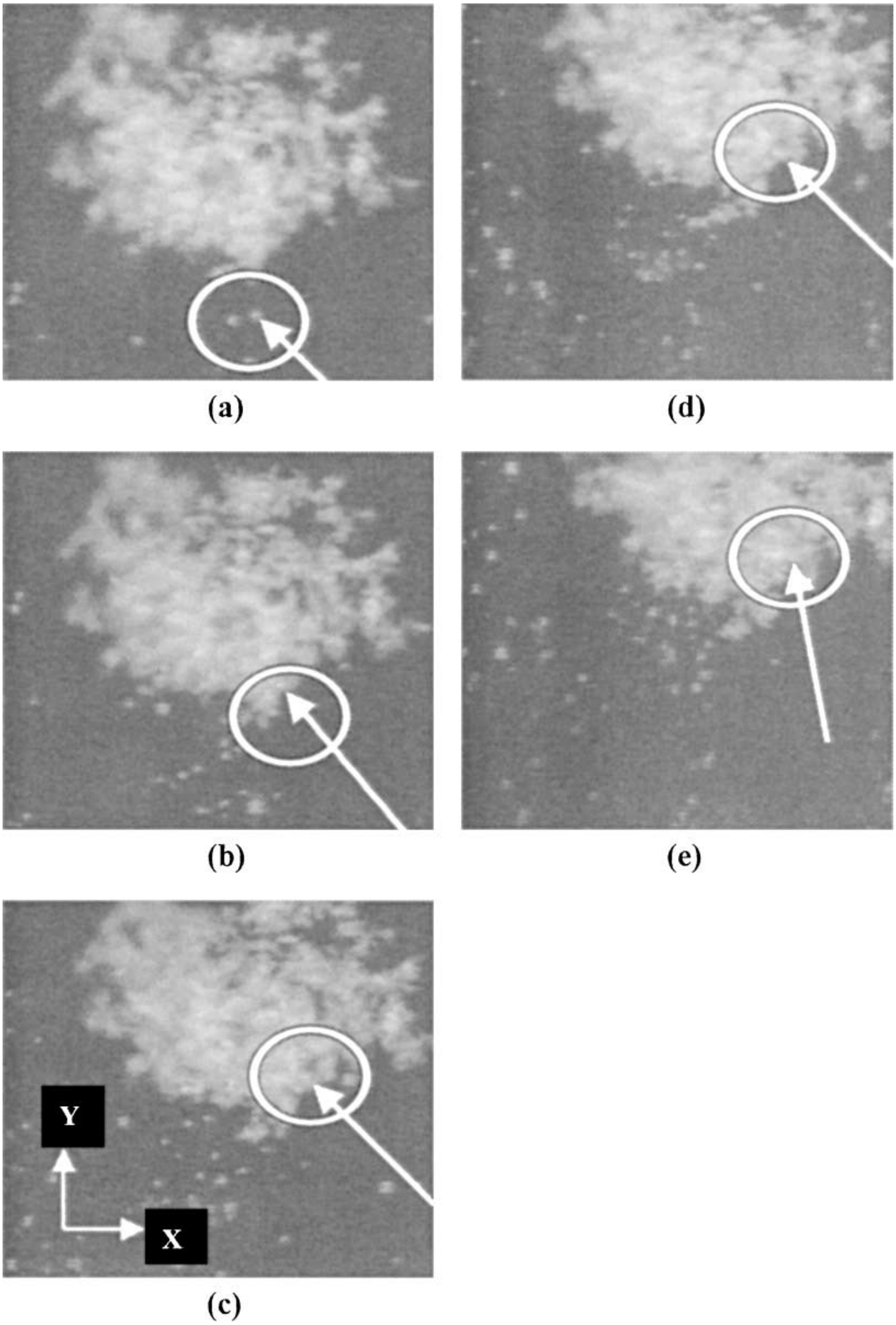

FIG. 3. Microphotographs of the original floc A1. Each film was taken 0.42 s after the proceeding one. (a) the bubble approaches the floc; (b)–(e) the bubble's movement into the floc.

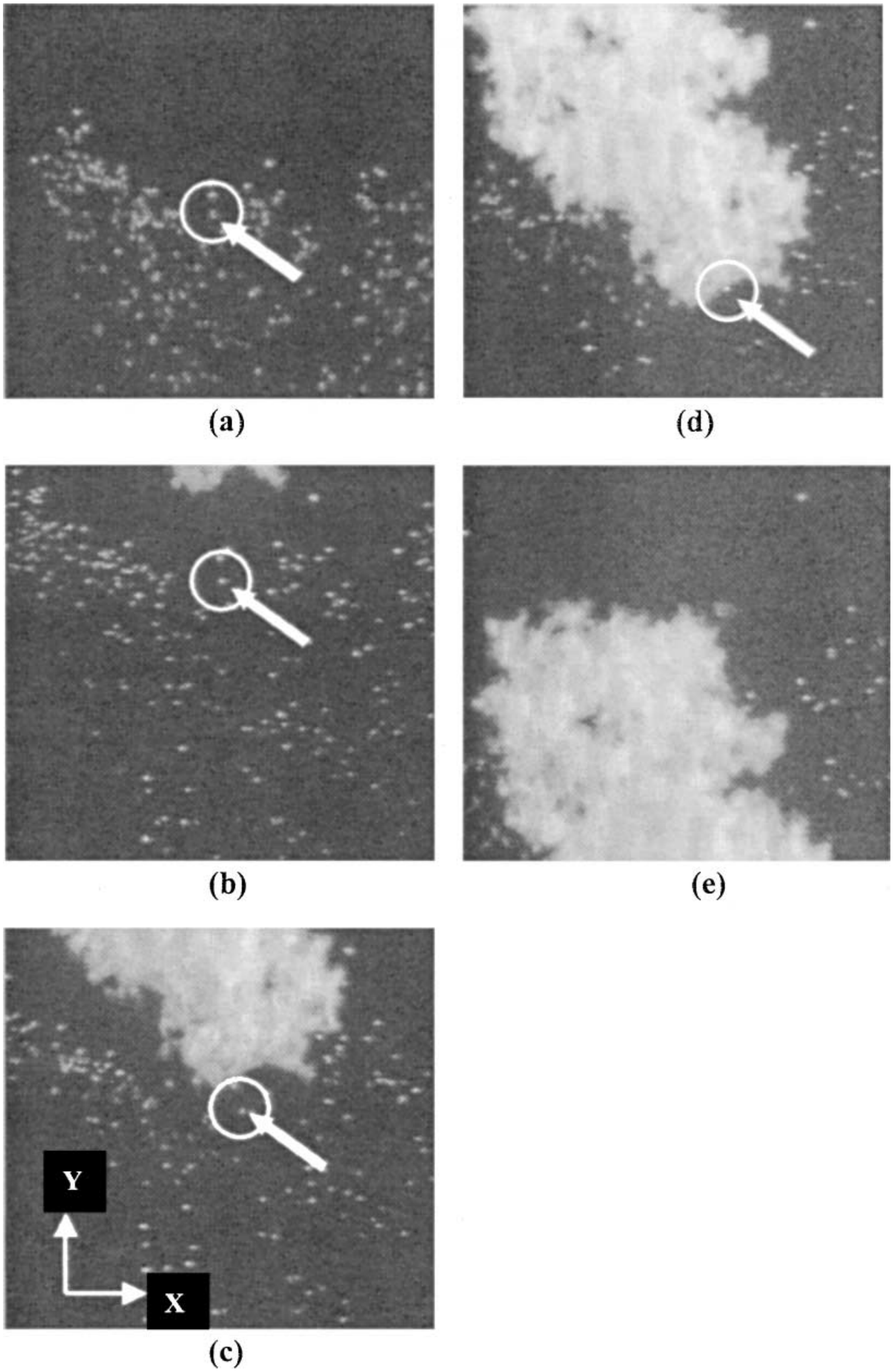

FIG. 4. Microphotograph of the original floc A4. Each film was taken 0.42 s after the proceeding one. (a, b) the bubble approaches the floc; (c)–(e) the bubble is pushed down by the floc.

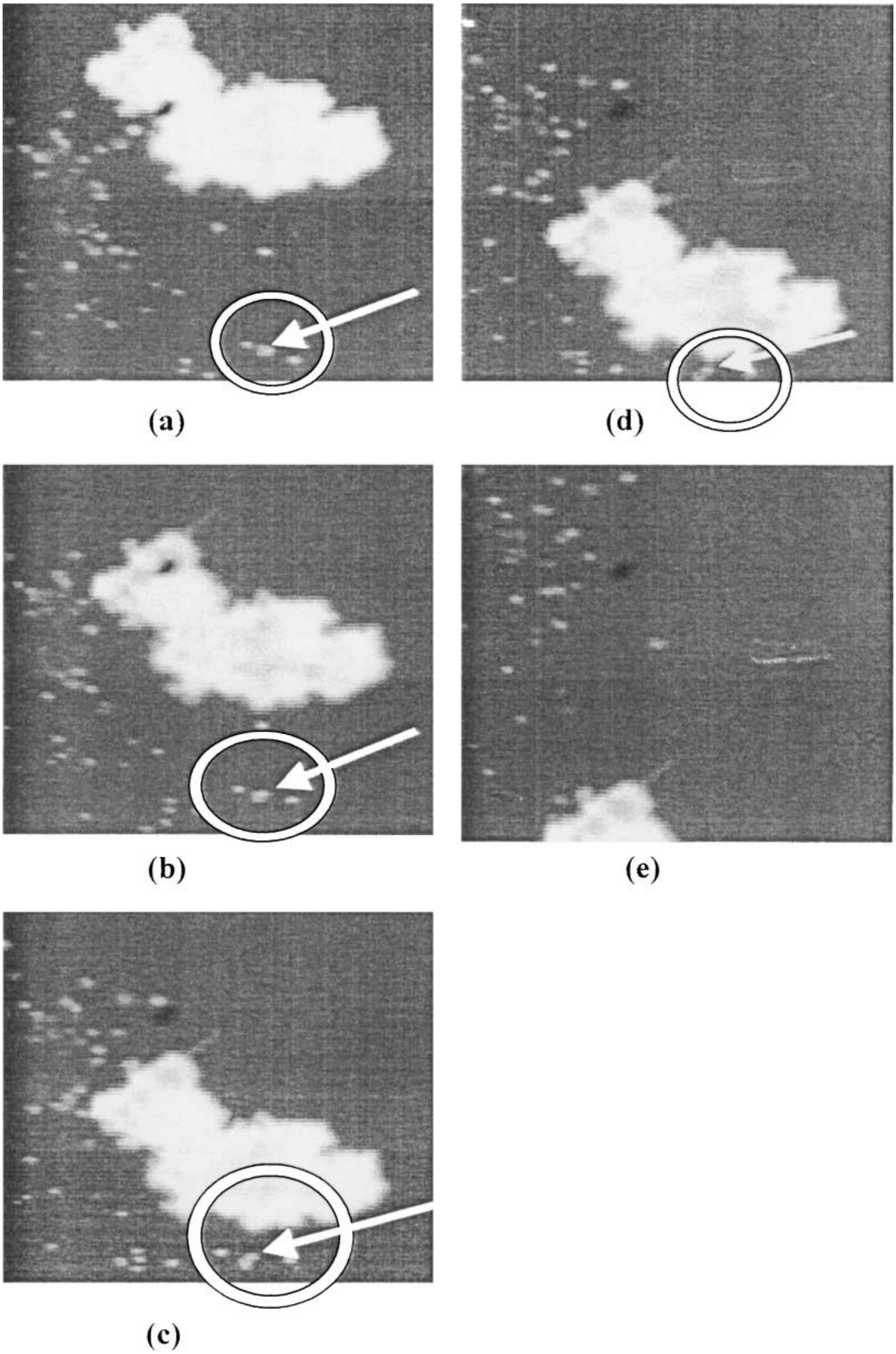

FIG. 5. Microphotograph of the original floc P4. Each film was taken 0.42 s after the proceeding one. (a, b) the bubble approaches the floc; (c)–(e) the bubble is pushed down by the floc.

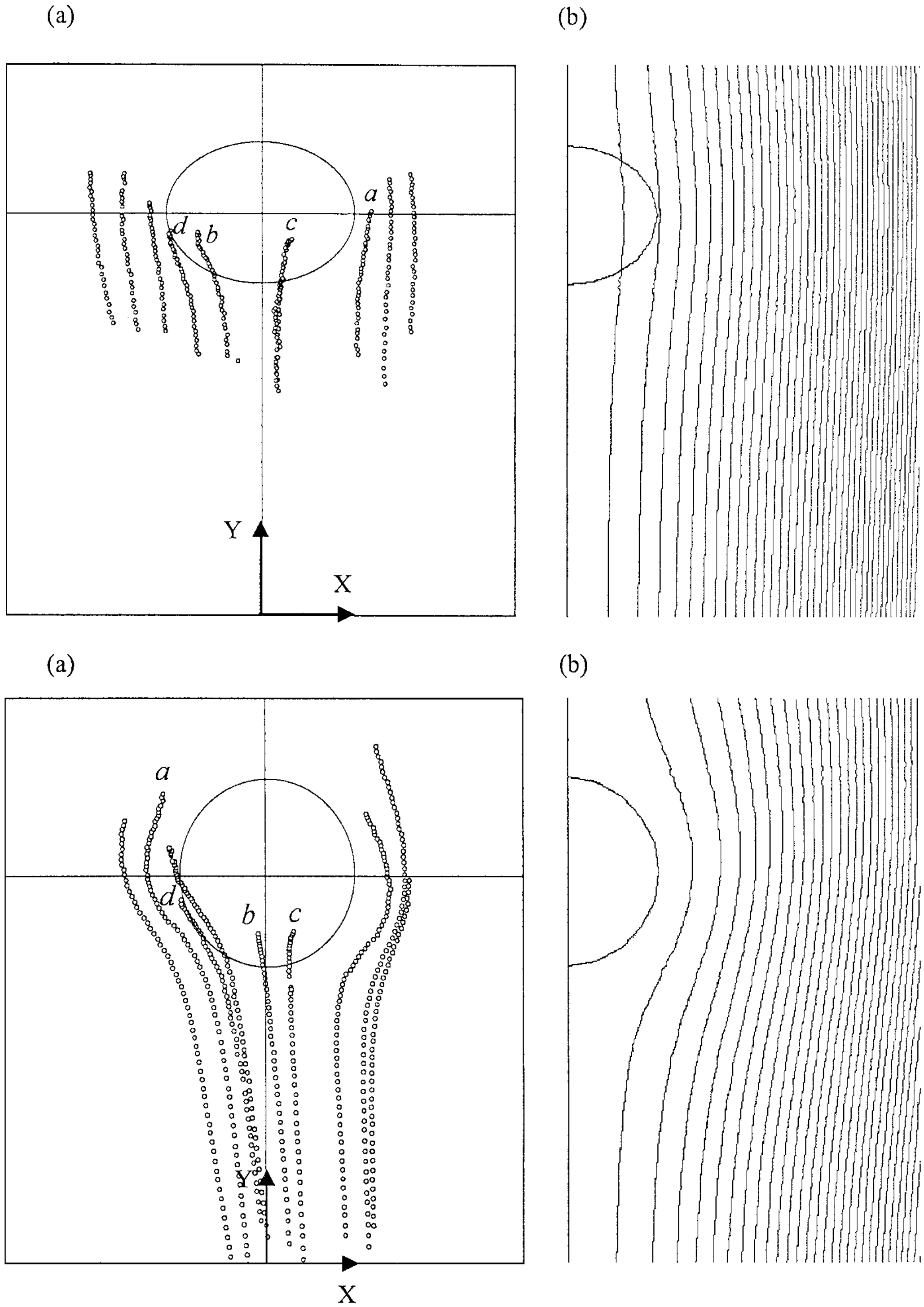

FIG. 6. Trajectories of the rising bubbles for each floc: (a) A1, (b) A4, and (c) P4. (left) Experimental observations; (right) numerical solutions.

Capture Ratio and Interior Permeability

The positions of the rising bubbles in relation to the floc can be obtained by simply subtracting the position vectors of the bubbles from that of the floc at different times. Figures 6a–6c summarize the positions of the hydrogen bubbles, relative to the falling flocs A1, A4, and P4. For comparison sake, the numerical solutions of flow fields with scheme by Wu and Lee (21) are also depicted in these figures. Reasonable agreement is noted between experiments and the simulations.

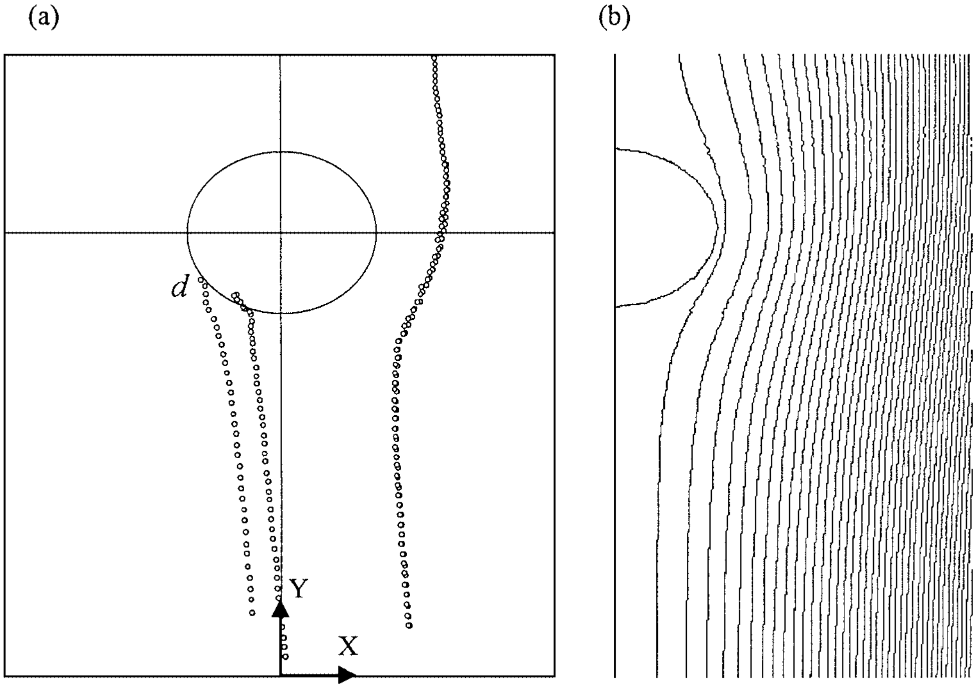

FIG. 6—*Continued*

Bubbles still change the direction in which they rise and approach the floc A1. Therefore, the floc's interior cannot be considered to be completely void as the presence of the floc interferes with the approach of the bubbles. For example, the bubble labeled *a* in Fig. 6a has been pushed outward when moving across the floc. Furthermore, the bubbles labeled *b* and *c* have simply penetrated the floc. Bubble *d* is particularly important, just sweeping over the floc surface as it passes, following the critical streamline depicted in Fig. 1. Tracking the motion of this bubble enables the ratio, ω/R, shown in Fig. 1, to be estimated as 0.73. That is, around 53% (0.73^2, $=\eta$) of the approaching fluid flows through the floc, revealing the significance of advection flow. Applying Adler's equation (Eq. [1]) with $\eta = 0.53$ yields a β value of 1.83, corresponding to the authors' previous estimate (10) of 1.2–3.1 for original sludge flocs. Li and Ganczarczyk (3) defined a critical β value of 10.9, below which the floc could be considered permeable. Therefore, A1 is a permeable floc with a permeability of 7.2×10^{-8} m^2. Table 1 presents estimated η and β values.

TABLE 1
Floc Characteristics

ID number	Diameter (μm)	V_t (mm/s)	Re_t	$\eta(-)$	$\beta(-)$
A1	985	0.13	0.13	0.53	1.83
A4	1,430	1.18	1.69	0.003	41.9
P4	1,310	2.48	3.25	0.12	5.3

Figure 6b shows the bubbles' trajectories around floc A4. Notably, the distortion of the trajectories of most bubbles exceeds that of A1. The approaching bubbles, labeled *b* and *c*, are just below the floc and appear to hit it. However, in fact rather than actually hitting the floc, they are pushed down and move together with the floc. The bubble sweeps over the surface of the floc (labeled *d* in Fig. 6b) and ω/R is estimated to be 0.054. That is, only 0.3% of the approaching fluid flows through the floc. Restated, the interior of floc A4 is essentially impermeable. Adler's equation estimates the corresponding β value as 41.9, yielding a permeability of 2.9×10^{-10} m^2, or just 0.4% of that of floc A1. Floc A4 is impermeable to advection flow as the β value of floc A4 is less than the critical value of 10.9 proposed in Ref. (3).

Figure 6c demonstrates the bubble trajectories around floc P4. The critical radius ω/R is estimated at 0.35. Restated, about 12% of the approaching fluid flows through the floc. Therefore, Adler's equation estimates the β value at 5.3, matching the authors' earlier estimate (15) of 4.2–6.8 for flocculated sludge flocs. The permeability of P4 is 1.5×10^{-8} m^2, or around 20% of that of the floc A1. Although this floc has a β value that is less than the critical value of 10.9, proposed by Ref. (3), most bubbles fail to penetrate this floc, even though it has a β value that is less than the critical value of 10.9, proposed by Ref. (3). Thus, the critical β value presented in Ref. (3) overestimated the significance of advection flow through the floc. This work proposed that the critical β value for permeable flocs should be under 5.3.

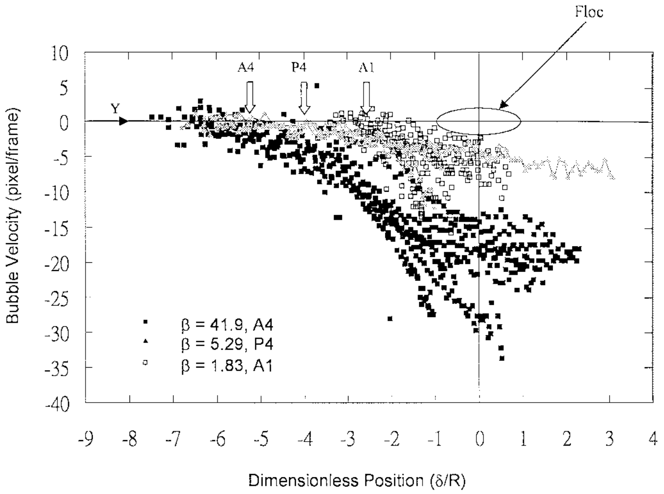

FIG. 7. Vertical component of $\mathbf{V}_{bf}$ versus the vertical distance between the centers of mass of the floc and the bubble.

Hydrodynamic Interactions

Tracking the positions of the floc and the rising bubbles enables their corresponding *relative* velocities to be numerically set using $\mathbf{V}_{bf} = \mathbf{V}_b - \mathbf{V}_f$. Figure 7 shows the vertical component of $\mathbf{V}_{bf}$ against the corresponding vertical distance between the centers of masses of the floc and the bubbles. The floc is represented by a circle whose center is at the origin of the axes, while the abscissa (X axis) specifies the bubble's location in numbers of floc radii away from the floc. When X is large and negative, the bubble is distant from the floc, and when $X = 0$, the bubble is at the same level as the floc, but does not necessarily hit the floc.

The fluid could "detect" the approach of a floc when the distance between it and the floc falls below a critical value, δ_c This critical distance for a porous floc is less than that for an impermeable floc, because of the advection flow (15). Figure 7 presents such a case. Flocs A1, A4, and P4 have δ_c values of around 2.1, 4.6, and 3.5 times the floc radius, respectively. This finding is consistent with the observed β sequence for these flocs: A1 < P4 < A4. Restated, a greater critical distance for flocs is associated with a higher β.

Additionally, the change in the vertical component of $\mathbf{V}_{bf}$ could be considered to measure the vertical force exerted on the bubbles by the floc. Notably, the floc exerted the greatest force on the bubbles at around one floc radius in front of its center of mass.

CONCLUSIONS

The fluid field surrounding sludge flocs was directly observed and the advection flow through the floc was noted. Closely examining the interactions between the motion of the free-falling floc and the rising bubbles revealed that around 53% of the approaching fluid flowed into an original activated sludge floc. The polyelectrolyte flocculation yielded compact sludge flocs and reduced the extent of advection flow to about 12%. From Adler's equation (Eq. [1]), the β value of the original activated sludge was estimated at 1.83, while that for the flocculated floc was 5.3. A compact floc exerts a greater force on the surrounding fluid than a loose one.

ACKNOWLEDGMENT

National Science Council, Republic of China, financially supported this work.

REFERENCES

1. Li, D. H., and Ganczarczyk, J., *Environ. Sci. Tech.* **23,** 1385 (1989).
2. Jiang, Q., and Logan, B. E., *Environ. Sci. Tech.* **25,** 2031 (1991).
3. Li, D. H., and Ganczarczyk, J., *Water Environ. Res.* **64,** 236 (1992).
4. Li, D. H., and Ganczarczyk, J., *Biotechnol. Bioengng.* **35,** 57 (1990).
5. Lee, D. J., J Ch I Ch E **25,** 201 (1994).
6. Lee, D. J., and Hsu, Y. H., *Environ. Sci. Tech.* **28,** 1444 (1994).
7. Huang, H., *Clay Clay Miner.* **41,** 373 (1993).
8. Logan, B. E., and Hunt, J. R., *Biotechnol. Bioengng.* **31,** 92 (1988).
9. Li, D. H., and Ganczarczyk, J., *Water Res.* **22,** 789 (1988).
10. Lee, D. J., Chen, G. W., Liao, Y. C., and Hsieh, C. C., *Water Res.* **30,** 541 (1996).
11. Masliyah, J. H., and Polikar, M., *Can. J. Chem. Eng.* **58,** 299 (1980).
12. Logan, B. E., and Hunt, J. R., *Limnol. Oceanogr.* **32,** 1034 (1987).
13. Matsumoto, K., Suganuma, A., and Kunii, D., *Chem. Eng. Sci.* **33,** 1554 (1978).
14. Rogak, S. N., and Flagan, R. C., *J. Colloid Interface Sci.* **134,** 206 (1990).
15. Wu, R. M., Feng, W. H., Tsai, I. H., and Lee, D. J., *Water Environ. Res.* **70,** 1258 (1998).
16. Wu, R. M., Tsou, G. W., and Lee, D. J., *Adv. Environ. Res.* **4,** 163 (2000).
17. Wu, R. M., Tsou, G. W., and Lee, D. J., *Chem. Eng. J.* **80,** 37 (2000).
18. Logan, B. E., "Environmental Transport Processes." Wiley, New York, 1999.
19. Saleh, S., Thovert, J. F., and Adler, P. M., *AIChE J.* **39,** 1765 (1993).
20. Alder, P. M., *J. Colloid Interface Sci.* **81,** 531 (1981).
21. Wu, R. M., and Lee, D. J., *Water Res.* **32,** 860 (1998).